OPEN ACCESS Freely available online

PLOS ONE

Population Structure, Historical Biogeography and Demographic History of the Alpine Toad *Scutiger ningshanensis* in the Tsinling Mountains of Central China

Hongzhe Meng, Xiaochen Li*, Penghai Qiao

Co-Innovation Center for Qinba Regions' Sustainable Development, College of Life Sciences, Shaanxi Normal University, Xi'an, China

Abstract

Population genetic structure, historical biogeography and historical demography of the alpine toad *Scutiger ningshanensis* were studied using the combined data mtDNA cytochrome b (cyt b) and the mtDNA cytochrome c oxidase subunit I (COI) as the molecular markers. This species has high genetic variation. There was a significant genetic differentiation among most populations. Three lineages were detected. The phylogenetic relationship analyses and the SAMOVA (spatial analysis of molecular variance) results showed significant phylogeographic structure. 82.15% genetic variation occurred among populations whereas differentiation within populations only contributed 17.85% to the total. Mantel test results showed a significant correlation between the pairwise calculated genetic distance and pairwise calculated geographical distance of the populations (regression coefficient $=0.001286$, correlation coefficient $=0.77051$, p $(r_{rand} \geq r_{obs}) = 0.0185 < 0.05$), indicating the existence of isolation-by-distance pattern of genetic divergence for cyt b + COI sequence, which suggests that the distribution of genetic variation is due to geographical separation rather than natural selection. The population expansion or contraction and genetic differentiation between populations or lineages could be explained by topography and the repetitive uplifts of the Tsinling Mountains and the climatic cycles during the late Pliocene and Pleistocene. *S. ningshanensis* experienced a rapid population expansion about 40,000 years before present. The current decline in population size was probably caused by anthropogenic disturbance. Current populations of *S. ningshanensis* are from different refugia though the location of these refugia could not be determined in our study. Topography, climatic changes and repetitive population expansion/contraction together led to the high level of genetic variation in *S. ningshanensis*. A total of three management units (MUs) was determined, which must be considered when conservation policy is made in the future.

Citation: Meng H, Li X, Qiao P (2014) Population Structure, Historical Biogeography and Demographic History of the Alpine Toad *Scutiger ningshanensis* in the Tsinling Mountains of Central China. PLoS ONE 9(6): e100729. doi:10.1371/journal.pone.0100729

Editor: Wolfgang Arthofer, University of Innsbruck, Austria

Received February 27, 2014; **Accepted** May 29, 2014; **Published** June 23, 2014

Funding: Funding was provided by the National Natural Science Foundation of China (No. 31071888). The funders had no role in study design, data collection and analysis, decision to publish, or preparation of the manuscript.

Competing Interests: The authors have declared that no competing interests exist.

* Email: xiaochen@snnu.edu.cn

Introduction

Population genetic structure refers to the geographical pattern of genetic diversity within or among populations. It could be influenced by gene flow, genetic drift, selection, mutation and recombination. Gene flow is caused by the movement of individuals from one population to another [1]. Estimation of the gene flow level allows conservation biologists to understand the relationships between populations and assess levels of genetic variation in order to evaluate the relative levels of conservation concern hierarchically across populations in a species. Genetic drift is the change in the frequency of a gene variant in a population due to random sampling [2]. http://en.wikipedia.org/wiki/Genetic_drift - cite_note-Masel_2011-1#cite_note-Masel_2011-1Genetic drift may lead to disappearance of gene variants and thereby reduce genetic diversity.

Phylogeography connects historical processes in evolution with spatial distributions [4]. Analysis of mitochondrial data promoted the empirical development of phylogeography [3]. The statistical phylogeography is one of the widely used approaches in phylogeography, which takes into account the stochasticity of genetic processes into demographic inference based on coalescent models for parameter estimation [4,5].

The Tsinling Mountains are located in the central part of China, stretching from west to east (Fig. 1). These Mountains are boundary between Oriental realm and Palaearctic realm according to the zoogeographical regions of China [6], and also the watershed for Yangtze River and Yellow River catchment areas, for climate, flora and fauna in China [7–9]. The Oriental and Palaearctic species congregate here forming a specific biotic province and containing rich animal and plant resources [10,11]. Like other regions in the northern hemisphere, the Tsinling Mountains experienced several glacial-interglacial cycles during Pleistocene [12–18]. The climate associated with Pleistocene glacial cycles in East Asia was likely mild and characterized by a mosaic of mountains [19,20]. The past climatic events, such as the Quaternary glaciation, are believed to have played an important role in forming the geographical pattern of the montane species and could leave the vestiges in geographical distribution of genetic diversity of population [21–26]. The founder effect during the postglacial population recovery causes a reduction in population genetic diversity [27,28], and the subsequent rapid population

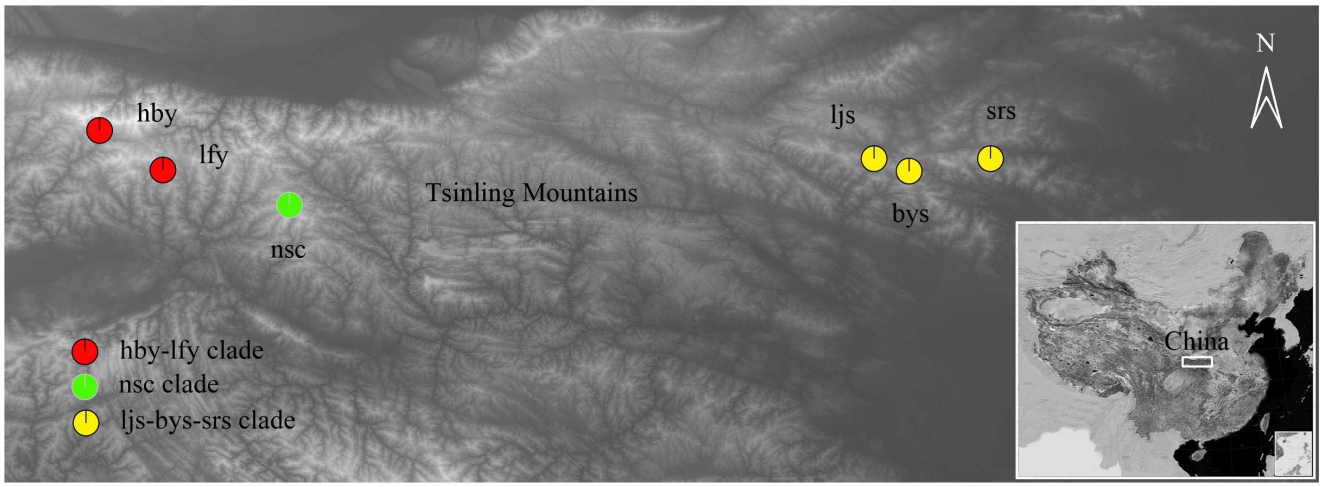

Figure 1. Locations of sampled populations and geographical distribution of *S. ningshanensis* clades on the Tsinling Mountains. Nsc is also the type locality of *S. ningshanensis*.
doi:10.1371/journal.pone.0100729.g001

expansion [29] may erase the previous geographical differences of the genetic diversity.

The alpine toad *Scutiger ningshanensis* was described from the western part of the Tsinling Mountains [30] (Fig. 1). Four years later, the second specimen of this species was collected from the same locality [31]. Since then, other specimen of this species was not collected until 2009 when some specimens were collected from several localities in the eastern part of the Tsinling Mountains [32]. Other than the reports on collection of additional specimens, only the biological characteristics of tadpoles of this species was studied [33]. The habitat of this species was roughly divided into two parts: the western part and the eastern part. Is this geographical pattern caused by habitat fragmentation or by populations from different glacial refugia? Does the isolation by distance between the local populations result in occurrence of any speciation events? The aims of the present study were to explore the population genetic structure, historical biogeography and the historical demography of *S. ningshanensis*.

Materials and Methods

Ethics statement

This study was approved by the Institutional Animal Care and Use Committee (IACUC) of Shaanxi Normal University. Only the clipped toes or tail tips of tadpoles were used for extraction of total DNA. No specific permissions were required for these locations/activities. This species was ranked "Endangered B2ab(iii)" in "The IUCN Red List of Threatened Species™ 2013" based on an outdated information that this species was only found at the type locality (nsc) [31] (http://www.iucnredlist.org). Actually, in addition to the type locality, this species was reported later in 2009 from a variety of localities including the Baiyunshan Mountains (bys), Shirenshan Mountains (srs) and Laojunshan

Table 1. Sampling information and haplotypes based on cyt b and COI for 6 sampled populations of *Scutiger ningshanensis*.

Population	Location	n	GPS coordinates	Elevation (m)	Haplotypes
hby	Huangbaiyuan, Taibai Co., Shaanxi Prov.	18	33.8749N 107.5168E	1652	hby1 (1), hby10 (1), hby12 (4), hby13 (1), hby14 (1), hby15 (1), hby16 (1),hby19 (1), hby2 (1), hby20 (1), hby3 (1), hby4 (1), hby7 (1), hby8 (1), hby9 (1)
lfy	Liangfengya, Foping Co., Shaanxi Prov.	17	33.6668N 107.8529E	2047	hby13 (1), lfy1(1), lfy10 (1), lfy12(2), lfy13 (1), lfy14 (1), lfy15 (1), lfy16 (1), lfy17 (1), lfy2(1), lfy3 (1), lfy4 (1), lfy5 (1), lfy6(1), lfy7 (1), lfy8(1)
nsc	Pingheliang, Ningshan Co., Shaanxi Prov.	15	33.4744N 108.5253E	2000	nsc1 (1), nsc10 (1), nsc11 (1), nsc12 (1), nsc13 (1), nsc14 (1), nsc15(1), nsc2 (1), nsc3 (1), nsc4(1), nsc5 (1), nsc6 (1), nsc7(1), nsc8 (1), nsc9 (1)
ljs	Laojunshan, Luanchuan Co., Henan Prov.	18	33.7272N 111.6309	1590	bys4 (6), ljs1 (4), ljs10 (2), ljs11 (1), ljs18 (1), ljs4 (1), ljs5 (2), ljs6 (1)
bys	Baiyunshan, Songxian Co., Henan Prov.	16	33.6535N 111.8283E	1675	bys1(8), bys10 (1), bys11 (2), bys14 (1), bys15 (1), bys4 (1), bys7 (2),
srs	Shirenshan, Lushan Co., Henan Prov.	15	33.7286N 112.2542E	1642	ljs11 (5), srs1 (3), srs15 (1), srs16 (1), srs17 (1), srs18 (1), srs5 (1), srs6 (1), srs9 (1)

n, sample size.
doi:10.1371/journal.pone.0100729.t001

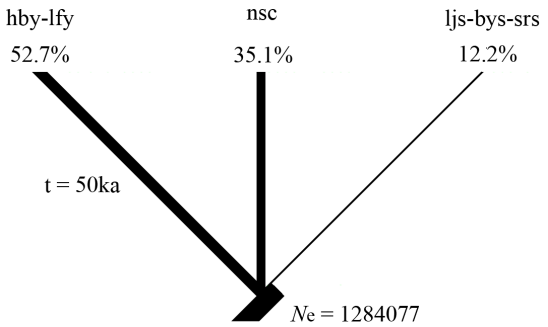

Figure 2. The model used to test the refugial hypotheses for *S. ningshanensis* using coalescent simulations. A single-refugium hypothesis concerning the refugia during the Dali glaciation (the last maximum glaciation in China which occurred about 50 ka before present) was tested. The detail interpretation for this model is given in the text. Branch lengths are time in generations based on a 6-year generation time in *S. ningshanensis*. Branch widths (effective population size, N_e) are scaled for each group based on the proportion of the total N_e that each group comprised.
doi:10.1371/journal.pone.0100729.g002

Mountains (ljs) [32] (Fig. 1), which indicated that this species doesn't meet the criteria of critically endangered or endangered defined in The IUCN Red List of Threatened Species™ 2013, therefore this species should be removed from the red list. However, the new data was not taken into account when this species was ranked "Endangered B2ab(iii)" in "The IUCN Red List of Threatened Species™ 2013". The specific location (GPS coordinates) of our study was given in Table 1.

Sampling and laboratory protocols

Our sampling covers the entire known distribution of this species. Furthermore, to make an extensive sampling, we explored the whole Tsinling Mountains, and fortunately collected this species at two locations where the distribution of this species has not been recorded. A total of 99 samples were collected from 6 localities during 2011 and 2013 (Table 1, Fig. 1). Eight samples of the alpine toad *Scutiger boulengeri* were collected from Jone County (34.539922N 103.491647E), southern Gansu Province, China. *S. boulengeri* will be used as outgroup in phylogenetic relationship analysis.

The clipped toes or tail tips of tadpoles were preserved in 100% ethanol and stored at −20°C. A continuous fragment (1009 bp) of the mitochondrial cytochrome b (cyt b) was amplified using PCR (MyCycler Thermal Cycler), with primers FrogGlu-f 5′-TGATCTGAAAAACCACCGTTG-3′ and FrogThr-r 5′-CTCCATTCTTCGRCTTACAAG-3′ [34]. A continuous fragment (631 bp) of the mitochondrial cytochrome c oxidase subunit I (COI) was amplified using PCR (MyCycler Thermal Cycler), with primers forward LepF5′-ATT CAA CCA ATC ATA AAG ATA TTG G-3′ and reverse LepR5′-TAA ACT TCT GGA TGT CCA AAA AAT CA-3′ [35]. The PCR products were purified using a purification kit (DC3511-02/3514-02 250 Preps, Biomiga, USA). Sequencing reactions were carried out with the PCR primers using ABI Prism BigdyeTM Terminator Cycle Sequencing Ready Reaction Kit on ABI 3730XL sequencer. All sequences have been deposited in the GenBank databases under accession numbers KF757340–KF757391 (*S. ningshanensis* cyt b), KF757392–KF757439 (*S. ningshanensis* COI); KJ082065–KJ082072 (*S. boulengeri* cyt b), KJ082073–KJ082080 (*S. boulengeri* COI). Indicators of nuclear mitochondrial pseudogenes (numts), such as indels, stop codons and double peaks in sequence chromatograms [36] were not found.

Determination of generation time

A skeletochronological study of longevity of *S. ningshanensis* was conducted. The clipped phalanges were stored in 95% ethanol solution. The phalanges were washed in running tap water, then decalcified in 3% nitric acid for 12 to 24 hours. The mid-diaphyseal region of the phalanges was cross-sectioned at 12–20 μm using a microtome and stained with hematoxylin for two min. Sections were examined under a light microscope and the number of lines of arrested growth (LAGs) was counted [37,38]. The number of LAGs represents the age of the toad.

Nucleotide polymorphism

The sequences were aligned with Clustal X1.83 [39]. The aligned sequences were edited using the program BioEdit 7.0.9.0 [40]. All analyses were performed based on the combined mitochondrial DNA data. Haplotype inference was conducted through Collapse 1.2 (http://darwin.uvigo.es). The number of variable and parsimony informative sites was determined using the program DnaSP 5.10.01 [41], and haplotype diversity (*Hd*) and nucleotide diversity (*Pi*) were determined through Arlequin 3.5.1.2 [42].

Phylogenetic analyses

The substitution model selection was implemented in jModelTest 2.1.4 [43], the TIM2+I+G model was selected for all datasets by likelihood ratio tests either under the Akaike Information Criterion (AIC) or under the Bayesian Information Criterion (BIC). Bayesian inference (BI) was used to generate a phylogenetic hypothesis of the DNA haplotypes. BI was performed in MrBayes

Table 2. Genetic diversity of each population of *S. ningshanensis*.

Population	Haplotype diversity ± *S.D.*	Mean number of pairwise differences ± *S.D.*	Nucleotide diversity ± *S.D.*
hby	0.9591±0.0359	20.187135±9.337776	0.012309±0.006363
lfy	0.9917±0.0254	14.416667±6.820745	0.008791±0.004658
nsc	1.0000±0.0243	8.876190±4.336499	0.005412±0.002965
ljs	0.8498±0.0426	1.928854±1.137129	0.001176±0.000773
bys	0.7500±0.1071	2.091667±1.231968	0.001275±0.000841
srs	0.9333±0.0773	3.044444±1.729647	0.001856±0.001193
Total population	0.9825±0.0055	41.822511±18.302675	0.025502±0.012361

S.D., standard deviation.
doi:10.1371/journal.pone.0100729.t002

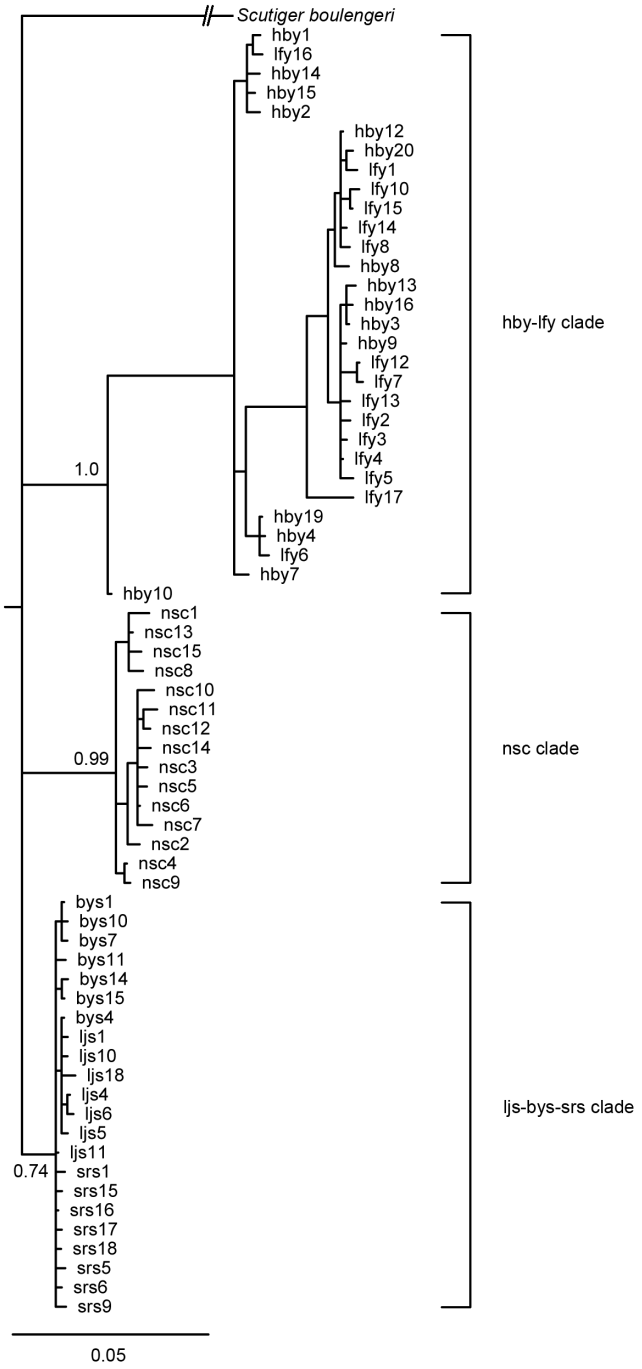

Figure 3. Bayesian tree for the 67 sampled haplotypes of *S. ningshanensis* based on the combined mtDNA cyt b and COI sequences. The Bayesian posterior probabilities from Bayesian analyses are presented above or under the main branches. The scale bar represents substitutions per site.
doi:10.1371/journal.pone.0100729.g003

3. 2 [44] with 1,200,000 generations, sampling trees every 100 generations. Two independent runs each with four simultaneous Monte Carlo Markov chains (MCMC) were conducted. The first 25% of generations were discarded as 'burn-in'. The convergence of chains was confirmed until average standard deviation of split frequency is below 0.01 (0.009889) and the potential scale reduction factor (PSRF) is close to 1.0 for all parameters. In phylogenetic analysis *S. boulengeri* was used as outgroup.

Population structure analyses

The population comparisons using pairwise difference as distance method, and the partition of genetic diversity within and among populations were analyzed by analysis of molecular variance (AMOVA) [45] using Arlequin3.5.1.2 [42] with 10,000 permutations. Mantel tests [46] were also conducted in Arlequin3.5.1.2 to assess the significance of isolation by distance (IBD) between populations with 10,000 random permutations on matrices of pairwise population F_{ST} values and the geographical distances. Pair-wise F_{ST} values between populations were estimated using Arlequin3.5.1.2, while geographical distances between populations were calculated online at http://www.gpsvisualizer.com/calculators#distance.

The spatial genetic structure of haplotypes was analyzed using the program SAMOVA1.0 [47] (http://web.unife.it/progetti/genetica/Isabelle/samova.html) with 1,000 permutations. The number of initial conditions was set to 100 as recommended by Dupanloup et al. [48]. The number K of groups of populations ranged from 2 to 4. The K with the highest Fct represents the best number of groups and the best population configuration.

Historical biogeography

The effective population size (N_e) of each clade (geographical group) for coalescent simulations was converted from Theta using the equation $\theta = N_e\mu$ with $\mu = 0.65\times10^{-8}$ (per lineage per million years) $\times6$ (generation time of *S. ningshanensis*). The θ-values were estimated using maximum likelihood method in the program Lamarc2.7.5 [48]. Total N_e was the sum of the N_e for all groups and the proportion of total N_e that each group comprised were used to scale the branch width of hypothesized trees (models of population divergence) (Fig. 2) [49–51]. Branch widths can be controlled by the Adjust Lineage Widths tool (the horizontal ruler) in the Tree Window in the program Mesquite2.75 [52].

A single-refugium hypothesis of population divergence during the Dali glaciation (the last maximum glaciation in China which occurred about 50 ka before present) was tested using the maximum likelihood estimation implemented in Mesquite2.75 [52] to infer the distributional area of the most recent common ancestor (MRCA) of clades. The single-refugium model hypothesizes that all current geographical populations derived from a single refugium at the end of the Dali glaciation and that all population divergences were concurrent and resulted from the fragmentation of a widely distributed common ancestor's range (Fig. 2). Branch lengths are time in generations based on a six-year generation time in *S. ningshanensis*. The clades were treated as taxon states and each haplotype as character states. The haplotype trees by coalescence within a diverging population tree (model of population divergence) were simulated, and fit of a haplotype tree to a population tree was calculated to search for population trees that optimize fit of gene trees.

Historical demography

Neutrality tests were calculated in Arlequin3.5.1.2 [41], Fu's F_S test [53] and Tajima's D [54] were used to detect evidence of recent demographic expansion within each inferred clade, under which negative value are expected [55]. Inference of population expansion events was performed using a mismatch analysis [56,57] using Arlequin3.5.1.2 with the number of bootstrap replicates set to 10,000 to explore the demographic history of the studied populations. A recent growth is expected to generate a unimodal distribution of pairwise differences between sequences [56]. The

Table 3. Results of analysis of molecular variance (AMOVA) of *S. ningshanensis*.

Source of variation	*d.f.*	Sum of squares	Variance components	Percentage of variation
Among populations	5	1646.756	19.92646 Va	82.15
Within populations	93	402.547	4.32847 Vb	17.85
Total	98	2049.303	24.25492	
Fixation Index: F_{st} = 0.82154 (*p*-value = 0.0±0.0)				

d.f., degrees of freedom.

doi:10.1371/journal.pone.0100729.t003

validity of the expansion model was tested using the sum of squared deviations (*SSD*) and Harpending's raggedness index (*R*) between observed and expected mismatches.

The site-frequency spectrum (for segregating sites) was calculated in DnaSP5.10.01 [41] to detect the excess of singleton mutations. The null hypothesis of the neutral model (constant population size) was rejected when the allelic frequency spectrum for the entire population revealed an excess of singleton mutations. The excess of singleton mutations could be caused by the expansion [58].

Furthermore, the Bayesian Skyline Plot (BSP) approach was used to estimate the demographic history in BEAST v1.8.0 [59]. The log file was analyzed in Tracer. Strict molecular clock model was selected based on the results from Tracer. A mean mutation rate of 0.65% change per lineage per million years was used [60–67]. Two independent BEAST runs from the same XML file were carried out and then the log output files were combined using LogCombiner. The combined log file was analyzed in Tracer to see if the Trace for each parameter has converged well on a stationary distribution.

Detection of cryptic species

To detect the existence of potential cryptic species, uncorrected p-distances [68,69] for all lineage pairs were calculated in PAUP4.0 [70] from all sequences. The average p-distances of all possible pairs of sequences (every sequence pair contains sequences from different lineages) were calculated.

Results

Generation time

The average longevity of tadpoles was estimated by Lu et al. [33]. The whole longevity equals the longevity of adult plus the longevity of tadpole. The average duration of the tadpole stage of *S. ningshanensis* is three years [33] and the average duration of the adult stage after metamorphosis is six years. The average life span of *S. ningshanensis* is nine years. The average generation time (GT) of *S. ningshanensis* is six years.

Genetic variation

A total of 107 samples were sequenced, including 99 samples of *S.ningshanensis* and eight of *S. boulengeri*. A total of 1009 base pairs of cyt b gene and 631 base pairs of COI gene was obtained, 67 haplotypes were identified for the combined gene sequences (cyt b+COI) of *S. ningshanensis*. Of the combined 1640 nucleotide sites, 181 were variable (polymorphic sites or segregating sites), 121 were parsimony informative, and 60 were singleton variable. The haplotype diversity of total and most sampled population was very high, however, the nucleotide diversity of every sampled population was low (Table 2). Among the total haplotypes, 82.09% are private haplotypes (Table 1).

Phylogenetic relationships among haplotypes

BI analysis revealed three distinct clades (lineages) (hby-lfy, nsc, ljs-bys-srs) in *S. ningshanensis*. Clades hby-lfy and nsc are well supported with posterior probabilities of 1 and 0.99. On the other hand clade ljs-bys-srs only has a posterior probability of 0.74 (Fig. 3). An important feature of these trees was that the components of each clade showed a strong geographical association. All haplotypes of clade hby-lfy were from western localities, all haplotypes of clade nsc were from locality nsc, all haplotypes of clade ljs-bys-srs were from the eastern localities (Fig. 1).

Population structure and genetic differentiation

AMOVA analysis suggested that majority of the variation occurred among populations (82.15%) while differentiation within populations only contributed 17.85% to the total (Table 3). The fixation index, a measure of population differentiation due to genetic structure, was highly indicating a significant genetic differentiation among populations (*p*-value = 0.0±0.0) (Table 3).

Table 4. F_{ST} values between populations.

Population	bys	hby	lfy	ljs	nsc	srs
bys	0.0					
hby	0.82921 (*p* = 0.0±0.0)	0.0				
lfy	0.89042 (*p* = 0.0±0.0)	0.06828 (*p* = 0.06851±0.002)	0.0			
ljs	0.38150 (*p* = 0.0±0.0)	0.84979 (*p* = 0.0±0.0)	0.90412 (*p* = 0.0±0.0)	0.0		
nsc	0.86254 (*p* = 0.0±0.0)	0.77573 (*p* = 0.0±0.0)	0.83417 (*p* = 0.0±0.0)	0.87731 (*p* = 0.0±0.0)	0.0	
srs	0.31488 (*p* = 0.0±0.0)	0.79976 (*p* = 0.0±0.0)	0.86822 (*p* = 0.0±0.0)	0.33801 (*p* = 0.0±0.0)	0.83596 (*p* = 0.0±0.0)	0.0

doi:10.1371/journal.pone.0100729.t004

Table 5. Geographical distances among populations.

Population	bys	hby	lfy	ljs	nsc	srs
bys	0.0					
hby	400.14	0.0				
lfy	368.7	38.76	0.0			
ljs	20.05	381.29	350.31	0.0		
nsc	307.33	103.54	65.98	289.6	0.0	
srs	40.36	438.94	408.07	57.77	347.22	0.0

doi:10.1371/journal.pone.0100729.t005

Population comparisons showed a significant genetic differentiation (F_{ST}) between most local populations except the population comparison between hby and lfy (Table 4).

Mantel test results showed a significant correlation between the pairwise calculated genetic distance and pairwise calculated geographical distance (Table 5) of the populations (regression coefficient $=0.001286$, correlation coefficient $=0.77051$, p ($r_{rand} \geq r_{obs}$) $=0.0185<0.05$), indicating the existence of isolation-by-distance pattern of genetic divergence for cyt b+COI sequence, which suggests that the distribution of genetic variation is due to geographical separation rather than natural selection. The Mantel test results provided the evidence for large-scale geographical population structure in this species.

Results from SAMOVA analysis indicated that the highest F_{CT} equals to 0.84285 (p (rand.value $\geq$ obs.value) $=0.01662\pm0.0$) when $K=3$, showing that the most likely number of populations is three.

Historical biogeography

The observed value of s is 55 which doesn't fall within the model of single-refugium indicating that the fragmentation model of population divergence was rejected (Fig. 4), that is, the current three lineages were derived from multiple refugia.

Demographic history

The results of mismatch distribution showed that the p-values for *SSD*s and *R*s of the total population and all clades were larger than 0.05, indicating a stable population size in the past; moreover, mismatch distribution in the total population and the clade hby-lfy showed frequency distribution of pairwise difference with multiple peaks (Fig. 5), on the other hand, the p-values for Tajima's D of total population, clade hby-lfy and clade nsc were larger than 0.05 also indicating a stable population size in the past. However, the p-values for Fu's F_Ss of all clades were smaller than 0.01, and the p-values for Tajima's D of clade ljs-bys-srs was smaller than 0.05, indicating all clades experienced a sudden population expansion (Table 6); on the other hand, mismatch distribution in clades nsc and ljs-bys-srs showed frequency distribution of pairwise difference with single peak (Fig. 5), indicating an sudden population expansion in the past. The two statistics, Tajima's D value and the Fu's F_S, are sensitive to

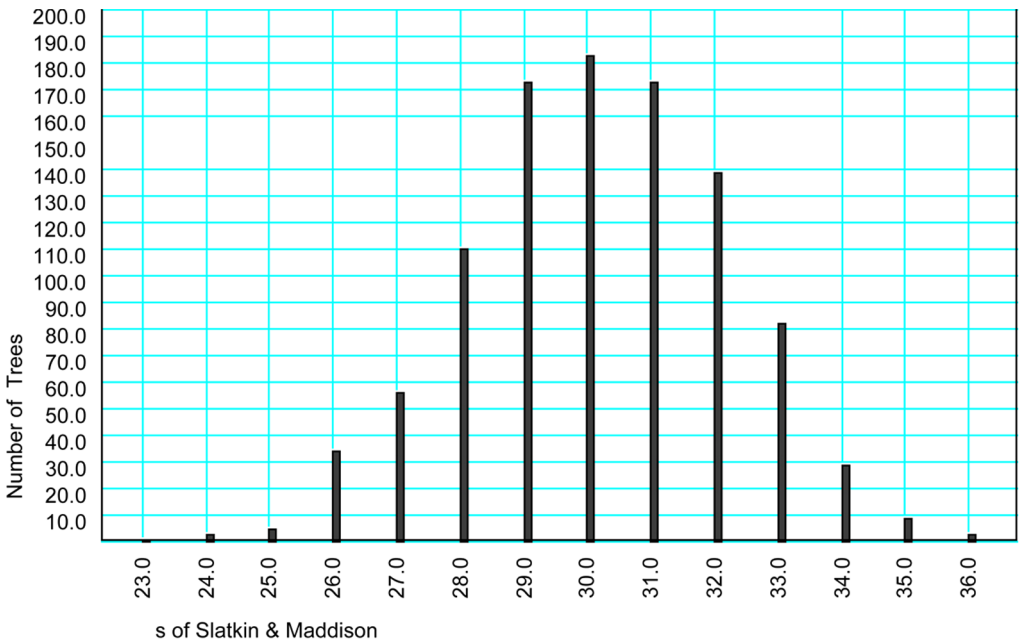

Figure 4. Distribution of *s*-values from simulated genealogies constrained within the models of population divergence. Single-refugium hypothesis.
doi:10.1371/journal.pone.0100729.g004

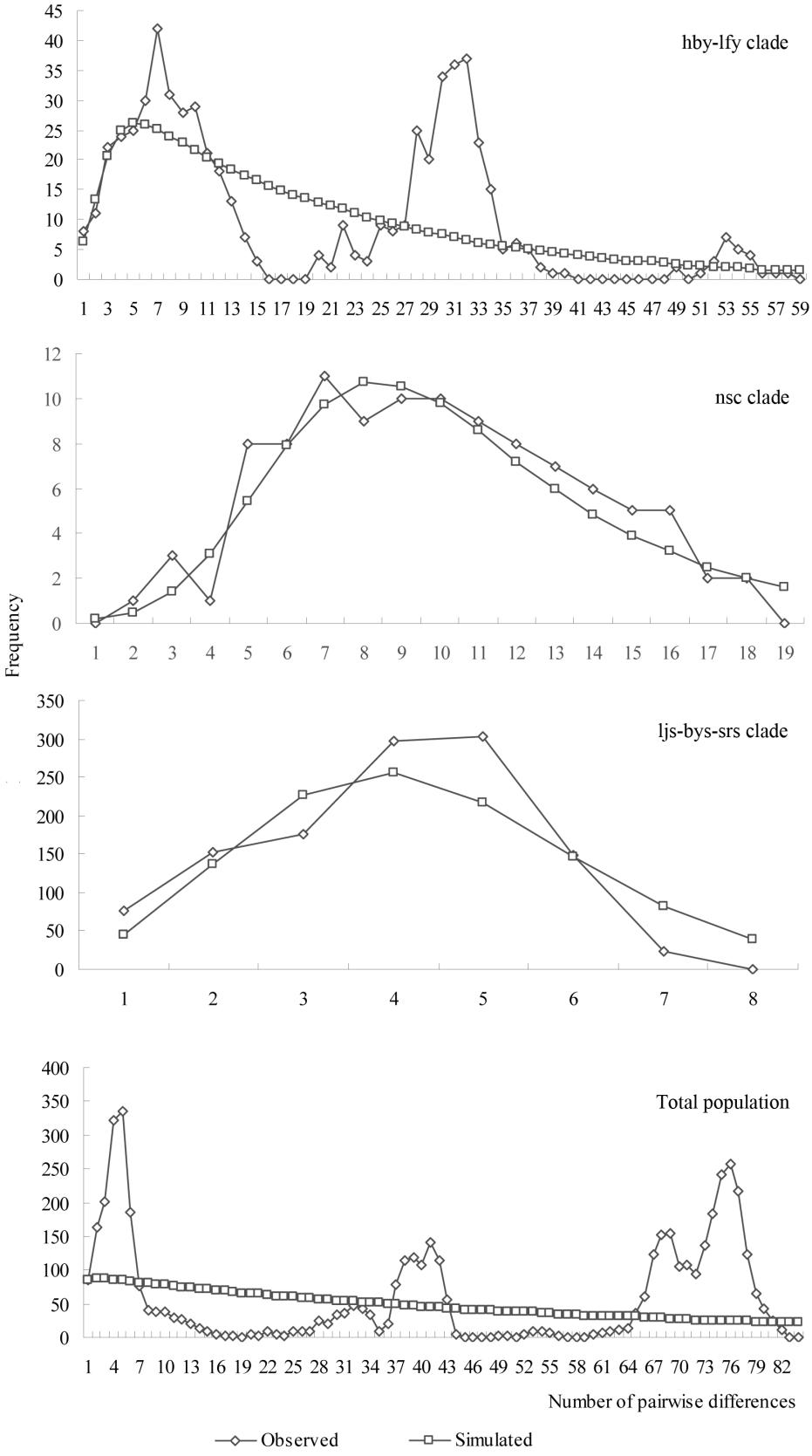

Figure 5. Mismatch distribution analysis for the total population and the clades.
doi:10.1371/journal.pone.0100729.g005

Table 6. Mismatch distribution analyses and neutrality test of *S. ningshanensis*.

Clade	*N*	*n*	τ (CI = 95%)	θ_0	θ_1	*SSD* (*p* value)	*R* (*p* value)	Fu's F_S (*p* value)	Tajima's *D* (*p* value)
hby-lfy	35	30	2.055 (0.0–35.352)	18.251	210.625	0.015 (0.5562)	0.005 (0.8915)	−9.08185 (0.0077)	−1.0915 (0.1265)
nsc	15	15	5.918 (2.23–16.926)	3.964	687.5	0.0024 (0.9685)	0.0082 (0.9791)	−8.12477 (0.0013)	−1.26501 (0.0931)
ljs-bys-srs	49	22	3.412 (1.396–4.701)	0.002	150.625	0.012 (0.0613)	0.044 (0.1165)	−13.343 (0.0)	−1.54633 (0.0402)
Total population	99	67	0.05859 (0.0–683.082)	53.204	99999.0	0.0219 (0.5223)	0.0044 (0.4604)	−7.80718 (0.0919)	0.64981 (0.8114)

N, number of sequences; *n*, number of haplotypes; τ, time in number of generations elapsed since the sudden expansion episode; θ_0, pre-expansion, and θ_1, post-expansion population size; *SSD*, sum of squared deviations; *R*, raggedness indexes.

doi:10.1371/journal.pone.0100729.t006

bottleneck effects or population expansion which leads to the more negative values of Tajim's *D* and Fu's F_S [71–74].

The allelic frequency spectrum for the entire population and all clades revealed an excess of singleton mutations and doesn't fit the neutral model (Fig. 6). The excess of singleton mutations could be caused by the expansion [58].

Bayesian skyline plot (BSP) further estimated the demographic history. The effective sample size (ESS) for all parameters of the BSP was greater than 200, showing that the 20 million generations were sufficient to determine the demographic history for each examined lineage. All lineages and the total population experienced population expansion. The hby-lfy lineage, nsc lineage and the total population experienced quick population growth after about 40,000 years ago, while the ljs-bys-srs lineage experienced a slow population growth after about 15,000 years ago. Noticeably, the hby-lfy lineage and the total population experienced a recent sharp decline in population, the ljs-bys-srs lineage showed a more recent population decline, while the nsc lineage maintained basically constant population size after the population expansion (Fig. 7).

Genetic distances between lingeages

The lineage hby-lfy and the lineage nsc were highly divergent from each other with an uncorrected p-distances of 4.2%, the lineage hby-lfy and ljs-bys-srs were also highly divergent with an uncorrected p-distances of 4.37%. Similarly, there was an high divergence between the lineage nsc and ljs-bys-srs, with an uncorrected p-distances of 2.37%. These values were similar to those p-distances (3%) reported between two different frog species [75]. Therefore *S. ningshanensis* probably contains three cryptic species or at least three subspecies.

Discussion

Genetic diversity

Our results showed high levels of genetic diversity in *S. ningshanensis*. High-level genetic diversity in narrowly endemic species could be associated with the factors such as the long species history, the high-level gene flow, having experienced a recent contraction in population, multiple founder events, the maintenance of genetic diversity in refugia, the hybridization, and the ability to survive in a range of different habitats. [76–78]. All these factors except hybridization might contribute to the high level of genetic diversity in *S. ningshanensis*. This species has probably undergone a long history through which many mutations were accumulated since their origin. High-level gene flow is beneficial to fix the mutations in population. Multiple founder events were another alternative explanation for the high-level genetic diversity in this species. There is a possibility that multiple founder events, which accumulated more and more mutations, occurred in the history of this species. The two congeners of *S. ningshanensis* are *S. boulengeri* and *S. liupanensis*. The nearest localities of these two species are 167 km or 361 km respectively away from the locality hby of *S. ningshanensis*, which makes it impossible for the occurring of hybridization among these three species [79,80]. Therefore, hybridization may not contribute to the high-level genetic diversity in *S. ningshanensis*. The distributing region of *S. ningshanensis* include a range of different habitats such as high mountains with different elevation, streams, and different vegetations. High-level diversity in habitats also contributed to the high-level genetic diversity.

Population structure

Significant population structure occured based on the statistics pairwise differentiation. Most pairwise F_{ST} values are high and

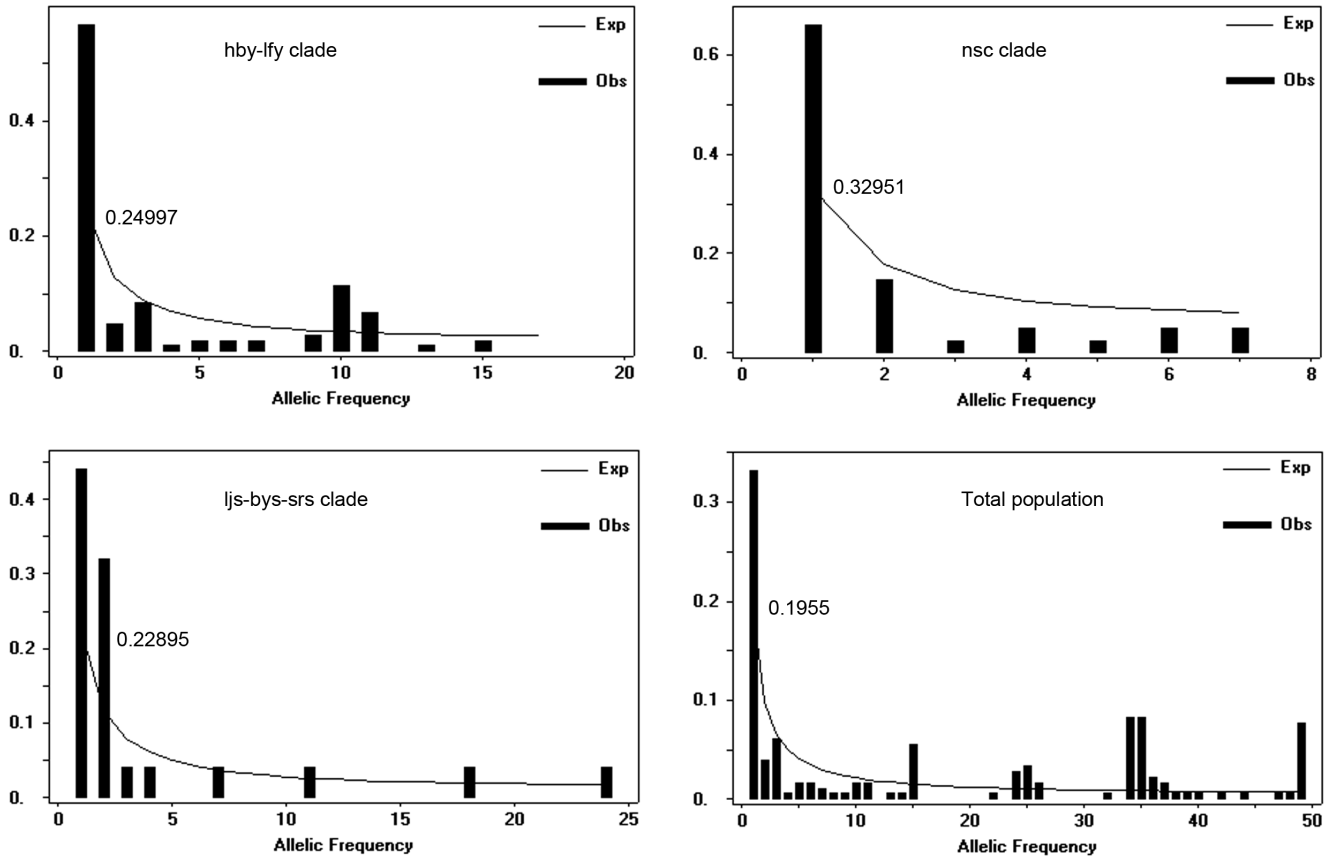

Figure 6. Allele frequency spectrum indicated an excess of singleton mutations in the combined mtDNA cyt b and COI sequences. Numbers above the line represent the number of sites with singleton mutations.
doi:10.1371/journal.pone.0100729.g006

statistically significant. Thus, the Ningshan alpine toad appears to exhibit substantial population differentiation across the Tsinling Mountains.

Mantel test results showed a significant correlation between the genetic distance and geographical distance of the populations, indicating the presence of IBD pattern of genetic divergence for cyt b+COI sequences, suggesting that the distribution of genetic variation is due to geographical separation rather than natural selection. The Mantel test results provided the clear evidence for large-scale geographical population structure in *S. ningshanensis*. It is not possible that a significant Mantel test provided the evidence for discontinuity in the distribution of genetic variation. It rather showed a continuous distribution of the variation due to individuals mating preferentially with individuals from nearby populations [81].

AMOVA results indicated that 82.15% genetic variation occurred among populations, while differentiation within the populations only made 17.85% contributions. The high genetic variation among populations affirmed the presence of phylogeographic structure in *S. ningshanensis*. SAMOVA results and the phylogenetic relationship analysis further affirmed the existence of phylogeographic structure in this species.

Amphibians have poor dispersal capabilities and are sensitive to fine-scale landscape structure, topographic and altitudinal variation and climatic changes [82–88]. Many amphibians are philopatric to breeding sites [89] which restricts gene flow and leads to significant genetic differentiation among populations and lineages.

Topography and Pleistocene climate changes drive population genetic differentiation forming genetic structure pattern [90–92]. East Asia including China has undergone a series of cooler-drier climate cycles in the last 15 million years [93]. Dramatic climatic changes have caused the extinction of many organisms [94]. *S. ningshanensis* that distributed in the areas with low elevation disappeared during the interglacial in the Quaternary since it is an alpine species. In addition, *S. ningshanensis* retreated to a few refugia during glacial period. At the end of the Dali glaciation, *S. ningshanensis* experienced a rapid population expansion which occurred about 40,000 years before present, and it is experiencing a population contraction now probably due to anthropogenic disturbance. Topographic features, climatic fluctuation and anthropogenic activity together led to the current patchy geographic pattern for *S. ningshanensis*. This geographical distribution pattern also seen in other montane organisms [95,96].

Finally, there is the possibility that unsampled populations between nsc and ljs may be genetically intermediate among the three groups.

Historical biogeography

The uplifts of the Tsinling Mountains promoted genetic differentiation among lineages of *S. ningshanensis*. The Tibetan Plateau experienced three phases of rapid uplifts [97,98]. The uplifts of the Tibetan Plateau impacted the environment of the surrounding areas including the Tsinling Mountains [97]. The Tsinling Mountains experienced similar uplift process, and three phases of uplifts occurred in Pliocene, Early Pleistocene and

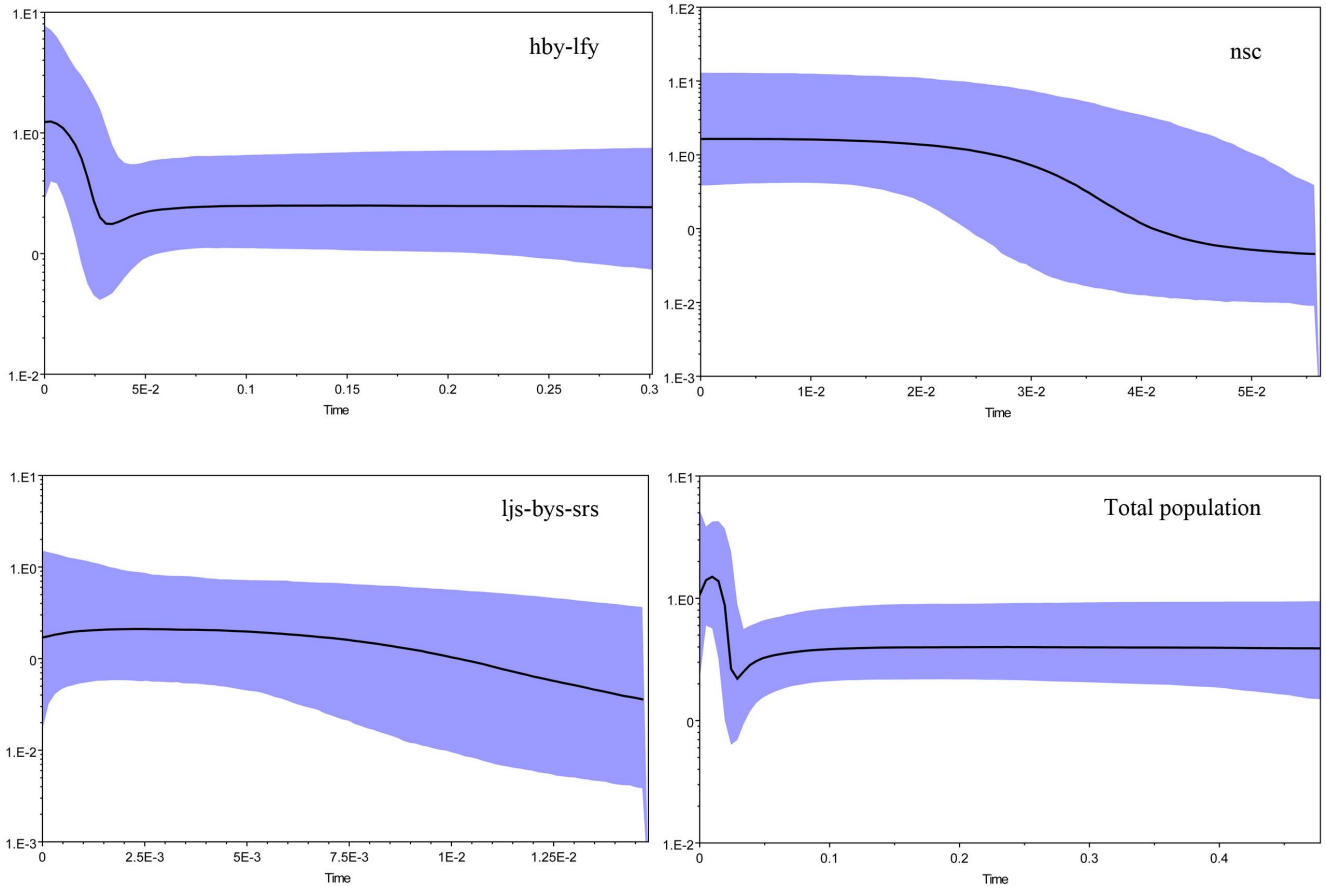

Figure 7. Demographic patterns of each clade and the total population as determined from the Bayesian skyline plot (BSP). The X-axis is in units of million years in the past and the Y-axis is N_e*μ (effective population size × mutation rate per site per generation). The median estimates for the log10 of the population size are shown as thick solid lines, and the 95% highest posterior density (HPD) limits are shown by the shaded areas.
doi:10.1371/journal.pone.0100729.g007

Holocene respectively [99–102]. Coalescent simulations indicated multiple refugia in *S. ningshanensis* though we could not determine the number and location of the refugia based on the statistical phylogeography analyses. Most species of the genus *Scutiger* inhabit in the eastern Tibetan Plateau [81], we guess that *S. ningshanensis* evolved when the *Scutiger* species dispersed eastward along the Tsinling Mountains. The hby-lfy lineage split apart at first, split between the lineages nsc and ljs-bys-srs occurred when this species continued dispersing from west to east on the Tsinling Mountains, while no further split occurred after the second split.

Demographic history

Most demographic analyses revealed a sharp population expansion in all lineages of *S. ningshanensis*, and the expansion began simultaneously 40,000 years before present, which corresponds to the end of the Dali glaciation. Retreat of glacier led to population expansion in species on the Tsinling Mountains. A noteworthy phenomena is that *S. ningshanensis* is experiencing a distinct recent population contraction (though the lineage nsc is exceptional) as shown by the BSP analyses (Fig. 7), there is a possibility that anthropogenic disturbance resulted in the contraction in population size of this species. Multiple uplifts of the Tsinling Mountains and fluctuations in population size of *S. ningshanensis* associated with glacial-interglacial cycles led to increases or decreases in the levels of genetic variation and coalescence times [23,25,28].

Putative cryptic species

S. ningshanensis probably contains at least two cryptic species or subspecies based on the p–distance analysis though there is not difference in morphology among these cryptic species or subspecies. The geographical distances between the local populations are long enough for occurrence of gene flow break in *S. ningshanensis* since it is philopatric to breeding sites. In addition, high peaks and deep valleys also contributed to the break of gene flow between populations. Subsequently, poor level of gene flow led to speciation events. However, there are limitations in taxonomic consequences based on only one taxonomic discipline. We will further confirm the cryptic speciation using data from nuclear DNA and ecological niche modeling (ENM) in the future.

Conservation and management implications

All potential cryptic species should be considered for conservation. Different conservation strategies should be accepted for different species, therefore, it is inappropriate to protect a cryptic species complex using a single conservation strategy [103]. It is indispensable to understand and quantify biodiversity so that we can better explain and at last carry out conservation [103]. The distribution area of this species is limited to a narrow zone along

the Tsinling Mountains, if this species is a cryptic species complex itself, the distribution area of each cryptic species is much smaller which increases the risk for extinction. Effective protection measures are to be provided and carried out. Conservation should be considered for every cryptic species.

Management units (MUs) are used to make conservation strategy for threatened species [104,105]. The three lineages (hby-lfy, nsc, ljs-bys-srs) derived from our study could be used as three different MUs, each MU has its own unique genetic structure. Every MU should be considered when conservation policy is made.

Conclusions

Three lineages were detected. The phylogenetic relationship analyses showed significant phylogeographic structure. The population expansion or contraction and genetic differentiation between populations or lineages could be explained by topography and the repetitive uplifts of the Tsinling Mountains and the climatic cycles during the late Pliocene and Pleistocene. *S. ningshanensis* experienced a rapid population expansion about 40,000 years before present. The current decline in population size was probably caused by anthropogenic disturbance. Current populations of *S. ningshanensis* are from different refugia though the location of these refugia could not be determined in our study. Topography is very important in shaping genetic connectivity. Topography, climatic changes and repetitive population expansion/contraction together led to the high level of genetic variation in *S. ningshanensis*. At least two putative cryptic species were detected. A total of three MUs were determined, which must be considered when conservation policy is made in future.

Acknowledgments

We are grateful to the academic editor Dr. Wolfgang Arthofer and the expert reviewer for their valuable comments which greatly improved the manuscript. We thank Mr. Meng, Shaanxi Normal University, for helping us collect samples. We want to express our gratitude to Dr. Xin-Ming Ma, Department of Neuroscience, University of Connecticut Health Center, Farmington, CT 06030-3401, U.S.A., for the English revision of the manuscript.

Author Contributions

Conceived and designed the experiments: XL. Performed the experiments: PQ HM. Analyzed the data: XL HM. Contributed reagents/materials/analysis tools: XL PQ HM. Wrote the paper: XL.

References

1. Slatkin M (1985) Gene flow in natural populations. Annu Rev Ecol Systemat 16: 393–430.
2. Masel J (2011) Genetic drift. Current Biol 21 (20): R837–R838.
3. Hickerson MJ, Carstens BC, Cavender-Bares J, Crandall KA, Graham CH, et al. (2010) Phylogeography's past, present, and future: 10 years after Avise, 2000. Mol Phylogenet Evol 54: 291–301.
4. Knowles L, Maddison W (2002) Statistical phylogeography. Mol Ecol 11: 2623–2635.
5. Knowles L (2009) Statistical phylogeography. Annu Rev Ecol Evol Syst 40: 593–612.
6. Zhang RZ, Zhao KT (1978) On the zoogeographical regions of China. Acta Zool Sin 24: 196–202. (in Chinese with English abstract)
7. Liu YH (1974) Natural geographical charateristics and utilization of Tsinling Mountains. J Shaanxi Norm Univ (Nat Sci Edit), (2): 74–83. (in Chinese)
8. Liu K, Ma NX, X YL, Sun GN (2004) Protection and construction of ecoenvironment in Qinling Mountainous area. Chinese J Ecol 23 (3): 157–160 (in Chinese with English abstract)
9. Ma CC (2007) A brief talk on Qinling's geographic significance. J Suzhou Univ 22 (4): 23, 109–110. (in Chinese with English abstract)
10. Zhang JL, Li HF (1997) Biodiversity in Tsinling natural reserve group. Chinese Biodiv 5: 155–156. (in Chinese)
11. Guo XR, Li ML, Zhuang SH (2000) A study on the diversity of Hemiptera insect in Huoditang forest farm. J Northwest Forestry Univ 15 (3): 71–75. (in Chinese with English abstract)
12. Wang GZ (1984) A sketch of Quaternary glaciation in eastern Qinling. Geol Shaanxi 2 (2): 47–62. (in Chinese with English abstract)
13. Liu YM, Wang GZ (1985) Research on Quaternary glacial geology in Qinling Mountain. Bull Tianjin Inst Geol Miner Resour 14: 1–104. (in Chinese with English abstract)
14. Ma QH, He YQ (1988) Moraine features and ice ages of the Quaternary in the Taibai Mountain. J Glaciol Geocryol 10: 66–75. (in Chinese with English abstract)
15. Tian ZS, Huang CC (1990) The glaciation process in Mt. Taibai of the Qinling Mountains and the climatic changes in the Loess Plateau. Geogr Res 9 (3): 15–23. (in Chinese with English abstract)
16. Xia ZK (1990) The ancient glacial relief and the faulting tectonics in the Taibaishan, Qinling Mts. J Glaciol Geocryol 12: 155–160. (in Chinese with English abstract)
17. Rost KT (1994) Geomorphological feature investigation of former and recent periglaciation in middle of Qinling Shan (P R China). J Xi'an College Geol 16 (2): 39–49.
18. Zhao ZZ, He PY (1997) Quaternary glacaition in Shennongjia. J Geomech 3 (2): 18–23. (in Chinese with English abstract)
19. Pinot S, Ramstein G, Harrison SP, Prentice IC, Guiot J, et al. (1999) Tropical paleoclimates at the Last Glacial Maximum: comparison of Paleoclimate Modeling Intercomparison Project (PMIP) simulations and paleodata. Climate Dynamics 15: 857–874.
20. Ju LX, Wang HJ, Jiang DB (2007) Simulation of the Last Glacial Maximum climate over East Asia with a regional climate model nested in a general circulation model. Palaeogeography, Palaeoclimatology, Palaeoecology 248: 376–390.
21. Avise JC (2000) Phylogeography. Harvard University Press, Cambridge, Massachusetts.
22. Carstens BC, Brunsfeld SJ, Dermboski JR, Good JM, Sullivan J (2005) Investigating the evolutionary history of the Pacific Northwest mesic forest ecosystem: hypothesis testing within a comparative phylogeographic framework. Evolution 59: 1639–1652.
23. Hewitt G (1996) Some genetic consequences of ice ages in divergence and speciation. Biol J Linn Soc 58: 247–276.
24. Hewitt G (1999) Post-glacial re-colonization of European biota. Biol J Linn Soc 68: 87–112.
25. Hewitt G (2000) The genetic legacy of the Quaternary ice ages. Nature 405: 907–913.
26. Taberlet P, Fumagalli L, Wust-Saucy AG, Cosson JF (1998) Comparative phylogeography and postglacial colonization routes in Europe. Mol Ecol 7: 453–464
27. Hayes JP, Harrison RG (1992) Variation in mitochondrial DNA and the biogeographic histories of woodrats (Neotoma) of the eastern United States. Syst Biol 41: 331–344.
28. Hewitt GM (2004) Genetic consequences of climatic oscillations in the Quaternary. Phil Trans R Soc B 359: 183–195.
29. Lessa EP, Cook JA, Patton JL (2003) Genetic footprints of demographic expansion in North America, but not in Amazonia, during the late Quaternary. Proc Natl Acad Sci USA 100: 10331–10334.
30. Fang RS (1985) A new species of *Scutiger* from Shaanxi, China. Acta Herpetologica Sinica 4 (4): 305–307. (in Chinese with English abstract)
31. Liang G, Lei FM, Fang RS (1989) The finding of *Scutiger ningshanensis* male (Anura: Pelobatidae). J Shaanxi Norm Univ (Nat Sci Edit) 17 (4): 92–93. (in Chinese with English abstract)
32. Chen XH, Li L, Jiang JP, Qiao L, Yang J (2009) Supplementary descriptions and geographic distribution of *Scutiger ningshanensis*, from Funiu Mountains, Henan, China. Acta Zootaxonomica Sinica 34 (3): 647–653. (in Chinese with English abstract)
33. Lu YY, Li PP, Liang G, Li A, Zheng ZY, et al. (2007) Biological characteristics of tadpoles of the Ningshan alpine toad *Scutiger ningshanensis* Fang, 1985. Acta Zool Sin 53 (2): 383–389. (in Chinese with English abstract)
34. Hillis DM, Mable BK, Larson A, Davis SK, Zimmer EA (1996) Nucleic acids IV: sequencing and cloning. In: Hillis DM, Mable BK, Moritz C (Eds.), Molecular Systematics, second ed. Sinauer, Sunderland, pp. 321–406.
35. Hebert PDN, Penton EH, Burns JM, Janzen DH, Hallwachs W (2004) Ten species in one: DNA barcoding reveals cryptic species in the neotropical skipper butterfly *Astraptes fulgerator*. Proc Natl Acad Sci USA 101: 14812–14817.
36. Song HJ, Buhay JE, Whiting MF, Crandall KA (2008) Many species in one: DNA barcoding overestimates the number of species when nuclear mitochondrial pseudogenes are coamplified. PNAS 105 (36): 13486–13491.
37. Kumbar SM, Pancharatna K (2001) Determination of age, longevity and age at reproduction of the frog *Microhyla ornata* by skeletochronology. J Biosci 26 (2): 265–270.
38. Üzüm N (2009) A skeletochronological study of age, growth and longevity in a population of the Caucasian Salamander, *Mertensiella caucasica* (Waga 1876) (Caudata: Salamandridae) from Turkey. North-Western J Zool 5 (1): 74–84.

39. Chenna R, Sugawarah H, Koike T, Lopes R, Gibson TJ, et al. (2003) Multiple sequence alignment with the Clustal series of programs. Nucl Acids Res 31: 497–500.
40. Hall TA (1999) BioEdit: a user-friendly biological sequence alignment editor and analysis program for Windows 95/98/NT. Nucl Acids Symp Ser 41: 95–98.
41. Librado P, Rozas J (2009) DnaSP v5: a software for comprehensive analysis of DNA polymorphism data. Bioinformatics 25: 1451–1452.
42. Excoffier L, Lischer HEL (2010) Arlequin suite ver 3.5: a new series of programs to perform population genetics analyses under Linux and Windows. Mol Ecol Resour 10: 564–567.
43. Darriba D, Taboada GL, Doallo R, Posada D (2012) jModelTest 2: more models, new heuristics and parallel computing. Nat Methods 9 (8): 772.
44. Ronquist F, Huelsenbeck JP (2003) MRBAYES 3: Bayesian phylogenetic inference under mixed models. Bioinformatics 19: 1572–1574.
45. Excoffier L, Smouse PE, Quattro JM (1992) Analysis of molecular variance inferred from metric distances among DNA haplotypes: Application to human mitochondrial DNA restriction data. Genetics 131: 479–491.
46. Smouse PE, Long JC, Sokal RR (1986) Multiple regression and correlation extension of the Mantel test of matrix correspondence. Syst Zool 35: 627–632.
47. Dupanloup I, Schneider S, Excoffier L (2002) A simulated annealing approach to define the genetic structure of populations. Mol Ecol 11: 2571–2581.
48. Kuhner MK (2006) LAMARC 2.0: maximum likelihood and Bayesian estimation of population parameters. Bioinformat Appl Note 22(6): 768–770.
49. Carstens BC, Sullivan J, Davalos LM, Larsen PA, Pedersen SC (2004) Exploring population genetic structure in three species of Lesser Antillean bats. Mol Ecol 13: 2557–2566.
50. Shepard DB, Burbrink FT (2008) Lineage diversification and historical demography of a sky island salamander, *Plethodon ouachitae*, from the Interior Highlands. Mol Ecol 17: 5315–5335.
51. Shepard DB, Burbrink FT (2009) Phylogeographic and demographic effects of Pleistocene climatic fluctuations in a montane salamander, *Plethodon fourchensis*. Mol Ecol 18: 2243–2262.
52. Maddison WP, Maddison DR (2011) Mesquite: a modular system for evolutionary analysis. Version 2.75, http://mesquiteproject.org.
53. Fu XY (1997) Statistical tests of neutrality of mutations against population growth, hitchhiking, and background selection. Genetics 147: 915–925.
54. Tajima F (1989) Statistical method for testing the neutral mutation hypothesis by DNA polymorphism. Genetics 123: 585–595.
55. Schneider S, Excoffier L (1999) Estimation of past demographic parameters from the distribution of pairwise differences when the mutation rates vary among sites: application to human mitochondrial DNA. Genetics 152: 1079–1089.
56. Rogers AR, Harpending H (1992) Population growth makes waves in the distribution of pairwise genetic differences. Mol Biol Evol 9: 552–569.
57. Rogers AR (1995) Genetic evidence for a Pleistocene population explosion. Evolution 49: 608–615.
58. Ramos-Onsins SE, Rozas J (2002) Statistical properties of new neutrality tests against population growth. Mol Biol Evol 19: 2092–2100.
59. Drummond A, Rambaut A (2007) BEAST: Bayesian evolutionary analysis by sampling trees. BMC Evol Biol 7: 214.
60. Moritz C, Dowling TE, Brown WM (1987) Evolution of animal mitochondrial DNA: Relevance for population biology and systematics. Annu Rev Ecol Evol S 18: 269–292.
61. Bermingham E, McCafferty SS, Martin AP (1997) Fish biogeography and molecular clocks: Perspectives from the Panamanian Isthmus. pp, 113–118 in Kocher TD and Stepien CA, (eds.), Molecular Systematics of Fishes. San Diego: Academic Press.
62. Macey JR, Schulte JA II, Larson A, Fang Z, Wang Y, et al. (1998a) Phylogenetic relationships of toads in the *Bufo bufo* species group from the eastern escarpment of the Tibetan Plateau: A case of vicariance and dispersal. Mol Phylogenet Evol 9: 80–87.
63. Macey JR, Schulte JA II, Ananjeva NB, Larson A, Rastegar-Pouyani N, et al. (1998b) Phylogenetic relationships among agamid lizards of the *Laudakia caucasia* species group: testing hypotheses of biogeographic fragmentation and an area cladogram for the Iranian Plateau. Mol Phylogenet Evol 10: 118–131.
64. Macey JR, Wang Y, Ananjeva NB, Larson A, Papenfuss TJ (1999) Vicariant patterns of fragmentation among gekkonid lizards of the genus *Teratoscincus* produced by the Indian Collision: A molecular phylogenetic perspective and an area cladogram for Central Asia. Mol Phylogenet Evol 12: 320–332.
65. Macey JR, Strasburg J, Brisson J, Vredenburg V, Jennings M, et al. (2001) Molecular phylogenetics of western North American frogs of the *Rana boylii* species group. Mol Phylogenet Evol 19: 131–143.
66. Weisrock DW, Macey JR, Ugurtas IH, Larson A, Papenfuss TJ (2001) Molecular phylogenetics and historical biogeography among salamandrids of the ''true'' salamander clade: rapid branching of numerous highly divergent lineages in Mertensiella luschani associated with the rise of Anatolia, Mol Phylogenet Evol 18: 434–448.
67. Wang B, Jiang J, Xie F, Li C (2012) Postglacial colonization of the Qinling Mountains: phylogeography of the swelled vent frog (*Feirana quadranus*). PLoS ONE, 7(7): e41579.
68. Takahashi K, Nei M (2000) Efficiencies of fast algorithms of phylogenetic inference under the criteria of maximum parsimony, minimum evolution, and maximum likelihood when a large number of sequences are used. Mol Biol Evol 17: 1251–1258.
69. Nei M, Kumar S (2003) Molecular evolution and phylogenetics. Oxford University Press, Oxford.
70. Swofford D (2002) PAUP*: Phylogenetic analysis using parimony (*and other methods). 4.0th edition. Sunderland, Massachusetts: Sinauer Associates.
71. Tajima F (1993) Measurement of DNA polymorphism. In 'Mechanisms of Molecular Evolution. Introduction to Molecular Paleopopulation Biology.' (Eds Takahata N & Clark AG) pp 37–59. Japan Scientific Societies Press, Sinauer Associates Inc: Tokyo, Sunderland, MA.
72. Tajima F (1996) The amount of DNA polymorphism maintained in a finite population when the neutral mutation rate varies among sites. Genetics 143: 1457–1465.
73. Aris-Brosou S, Excoffier L (1996) The impact of population expansion and mutation rate heterogeneity on DNA sequence polymorphism. Mol Biol Evol 13: 494–504.
74. Martel C, Viardb F, Bourguetc D, Garcia-Meuniera P (2004) Invasion by the marine gastropod *Ocinebrellus inornatus* in France. 1. Scenario for the source of introduction. J Experiment Marine Biol Ecol 305: 155–170.
75. Fouquet A, Gilles A, Vences M, Marty C, Blanc M, et al. (2007) Underestimation of species richness in Neotropical frogs revealed by mtDNA analyses. PLoS ONE 2, e1109.
76. Xue DW, Ge XJ, Hao G, Zhang CQ (2004) High genetic diversity in a rare, narrowly endemic primrose species: *Primula interjacens* by ISSR analysis. Acta Bot Sin 46 (10): 1163–1169.
77. Torres-díz CT, Ruizi E, González F, Fuentes G, Cavieres LA (2007) Genetic diversity in *Nothofagus alessandrii* (Fagaceae), an endangered endemic tree species of the coastal Maulino Forest of Central Chile. Ann Bot 100: 75–82.
78. Walker GF, Metcalf AE (2008) Genetic variation in the endangered *Astragalus jaegerianus* (Fabaceae, Papilionoideae): a geographically restricted species. Bull Southern California Acad Sci 107(3): 158–177.
79. Huang YZ (1985) A new species of pelobatid toads (Amphibia: Pelobatidae) from Ningxia Hui Autonomous Region. Acta Biol Plateau Sin 4: 77–81. (in Chinese with English abstract)
80. Fei L, Hu SQ, Ye CY, Huang YZ (2009) Fauna Sinica Amphibia Anura, volume 2. Beijing: Science Press.
81. Guillot G, Rousset F (2013) Dismantling the Mantel tests. Methods Ecol Evol 4 (4): 336–344.
82. Carey C, Bradford DF, Brunner JL, Collins JP, Davidson EW, et al. (2003) Biotic factors in amphibian population declines. In: Linder G, Krest SK, Sparling DW, eds.Amphibian Decline: An Integrated Analysis of Multiple Stressor Effects.Pensacola: Society of Environmental Toxicology and Chemistry Press. 153–208.
83. Collins JP, Storfer A (2003) Global amphibian declines: Sorting the hypotheses. Divers Distrib 9: 89–98.
84. Kraaijeveld-Smit FJ, Beebee TJ, Griffiths RA, Moore RD, Schley L (2005) Low gene flow but high genetic diversity in the threatened Mallorcan midwife toad *Alytes muletensis*. Mol Ecol 14: 3307–3315.
85. Murphy MA, Dezzani R, Pilliod DS, Storfer A (2010) Landscape genetics of high mountain frog metapopulations. Mol Ecol 19: 3634–3649.
86. Rowe G, Beebee T, Burke T (2000) A microsatellite analysis of natterjack toad, *Bufo* calamita, metapopulations. Oikos 88: 641–651.
87. Spear SF, Peterson CR, Matocq M, Storfer A (2005) Landscape genetics of the blotched tiger salamander (*Ambystoma tigrinum melanostictum*). Mol Ecol 14: 2553–2564.
88. Tallmon DA, Funk WC, Dunlap WW, Allendorf FW (2000) Genetic differentiation among long-toed salamander (*Ambystoma macrodactylum*) populations. Copeia 2000 (1): 27–35.
89. Blaustein AR, Wake DB, Sousa WP (1994) Amphibian declines: judging stability, persistence, and susceptibility of populations to local and global extinctions. Conserv Biol 8: 60–71.
90. Smith CI, Farrell BD (2005) Phylogeography of the longhorn cactus beetle *Moneilema appressum* LeConte (Coleoptera: Cerambycidae): was the differentiation of the Madrean sky islands driven by Pleistocene climate changes? Mol Ecol 14: 3049–3065.
91. Bryson RW, Murphy RW, Graham MR, Lathrop A, Lazcano D (2011a) Ephemeral Pleistocene woodlands connect the dots for highland rattlesnakes of the Crotalus intermedius group. J Biogeogr 38: 2299–2310.
92. Bryson RW, Murphy RW, Lathrop A, Lazcano-Villareal D (2011b) Evolutionary drivers of phylogeographical diversity in the highlands of Mexico: a case study of the *Crotalus triseriatus* species group of montane rattlesnakes. J Biogeogr 38: 697–710.
93. Axelrod D, Al Shehbaz I, Raven P (1998) History of the modern flora of China. Floristic characteristics and diversity of East Asian plants: proceedings of the first international symposium of floristic characteristics and diversity of East Asian plants: Springer Verlag Beijing: China. Higher Education Press.
94. Wang HW, Ge S (2006) Phylogeography of the endangered *Cathaya argyrophylla* (Pinaceae) inferred from sequence variation of mitochondrial and nuclear DNA. Mol Ecol 15: 4109–4122.
95. DeChaine EG, Martini AP (2004) Historic cycles of fragmentation and expansion in *Parnassius smintheus* (Papilionidae) inferred using mitochondrial DNA. Evolution 58: 113–127.

96. Yuan SL, Lin LK, Oshida T (2006) Phylogeography of the mole–shrew (*Anourosorex yamashinai*) in Taiwan: implications of interglacial refugia in a high-elevation small mammal. Mol Ecol 15: 2119–2130.
97. Li JJ, Fang XM, Pan BT, Zhao ZJ, Song YG (2001) Late Cenozoic intensive uplift of Qinghai-Xizang Plateau and its impacts on environments in surrounding area. Quaternary Sci 21(5): 381–391. (in Chinese with English abstract)
98. Pan BT, Gao HS, Li BY, Li JJ (2004) Step-like landform sand up lift of the Qinghai-Xizang Plateau. Quaternary Sci 24(1): 50–57. (in Chinese with English abstract)
99. Teng ZH, Wang XH (1996) Studying on the tectonic uplift of the Cenozoic era and the regional environmental effect s of the Qinling orogenic belt zone. Geol Shaanxi 14(2): 33–44. (in Chinese with English abstract)
100. Xue XX, Zhang YX (1996) The uplift stages and amplitudes of the Qinling Mountains by analyzing the distribution and character of the fossils found in the mountains. Geol Rev 42 (1): 30–36. (in Chinese with English abstract)
101. Xue XX, Li WH, Liu LY (2002) The northward shift of Weihe River and the uplift of Qinling Mountains. J Northwest Univ (Nat Sci Edit) 32(5): 451–454. (in Chinese with English abstract)
102. Xue XX, Li HH, Li YX, Liu HJ (2004) The new data of the uplifting of Qinling Mountains since the middle Pleistocene. Quaternary Sci 24 (1): 82–87. (in Chinese with English abstract)
103. Bickford D, Lohman DJ, Sodhi NS, Ng PKL, Meier R, et al. (2006) Cryptic species as a window on diversity and conservation. Trends Ecol Evol 22: 148–155.
104. Moritz C (1994) Defining 'evolutionarily significant units' for conservation. Trends Ecol Evol 9: 373–375.
105. Bidlack AL, Cook JA (2001) Reduced genetic variation in insular northern flying squirrels (*Glaucomys sabrinus*) along the North Pacific Coast. Anim Conserv 4: 283–290.